

LANDING GEAR FREE-FALL SIMULATION AND DAMPING OPTIMIZATION USING MATLAB

Mário Maia Neto, mario.neto@embraer.com.br¹

Luiz Carlos Sandoval Góes, goes@ita.br²

Rui Charles Mendonça Furtado, rui.furtado@embraer.com.br¹

¹Embraer Brazilian Aeronautical Company. Av. Brigadeiro Faria Lima, 2170, 12227-901, S.J. dos Campos, SP, Brazil.

²Aeronautical Institute of Technology, Department of Mechanical Engineering. Praça Marechal do Ar Eduardo Gomes, 50, 12228-900, S.J. dos Campos, SP, Brazil.

Abstract. *The airplane landing gear free-fall operation comprises a redundant, dissimilar and independent mechanically operated method of extending airplane landing gear due to a main hydraulic system failure or an electrical system malfunction. However, the emergency extension operation system design is not unique and spring-assisted, auxiliary hydraulics-assisted or even pneumatics-assisted landing gear free-fall design can be found in different airplanes. This paper aims at describing the model simulation and the optimization of certain parameters related to the associated hydraulic system, for the emergency operation condition, in a system configuration comprising simple extension by gravity (non-assisted system). Since the free-fall modeling involves different subjects like landing gear extension dynamics, hydraulic actuator kinematics, fluid mechanics and even aerodynamic drag, which illustrates the complexity behind its simulation and optimization, a deep literature review was accomplished in order to support all the formulation necessary to make the modeling feasible. Afterwards, some parametric models were created in MATLAB Simulink, which, by means of an iterative process, allowed the determination of specific parameters values that optimized the system damping for that operation. Parameters like restrictor orifices were evaluated for a chosen landing gear configuration and system performance optimized through the assistance of MATLAB optimization tools. Finally, the purpose of the optimum damping comprised the attenuation of the impact effects suffered by aircraft structure when landing gear falls by gravity in an emergency operation, as well as the assurance of sufficient energy for landing gear locking at the end of its downward movement.*

Keywords: *landing gear, free-fall, optimization, modeling, damping.*

1. INTRODUCTION

According to Currey (1998), the landing gear design comprises more engineering subjects than any other airplane design topic. Knowledge about materials, manufacturing processes, electrical and hydraulic systems, mechanisms and even runway strength is essential to make a good landing gear design.

The landing gear extension and retraction system choice is also a trade-off issue. While the electrical and hydraulic types are among the most used technologies for the normal landing gear operation system, the emergency extension system design is not also unique and spring-assisted, auxiliary hydraulics-assisted or even pneumatics-assisted landing gear free-fall design can be found in different airplanes. Generally, the airplane free-fall operation consists in a redundant, dissimilar and independent mechanically operated method of extending airplane landing gear due to a main hydraulic system failure or an electrical system malfunction. Operated by means of a lever or a knob, the system mechanically unlocks the landing gear and associated doors up locks, allowing landing gear to fall by gravity. The importance of the alternative extension system is related to the fact that a wheels-up landing may lead to fatal tragedies on several occasions.

The free-fall system to be modeled represents a simple configuration system, in which the landing gear down locking, normally accomplished by mechanical locks, will be guaranteed through the landing gear coming to its extended position with a satisfactory kinetic energy level, resultant from the combination of its falling by gravity into the aerodynamic flow and the existing resistance to its movement. Figure 1 presents the schematics of the system under analysis.

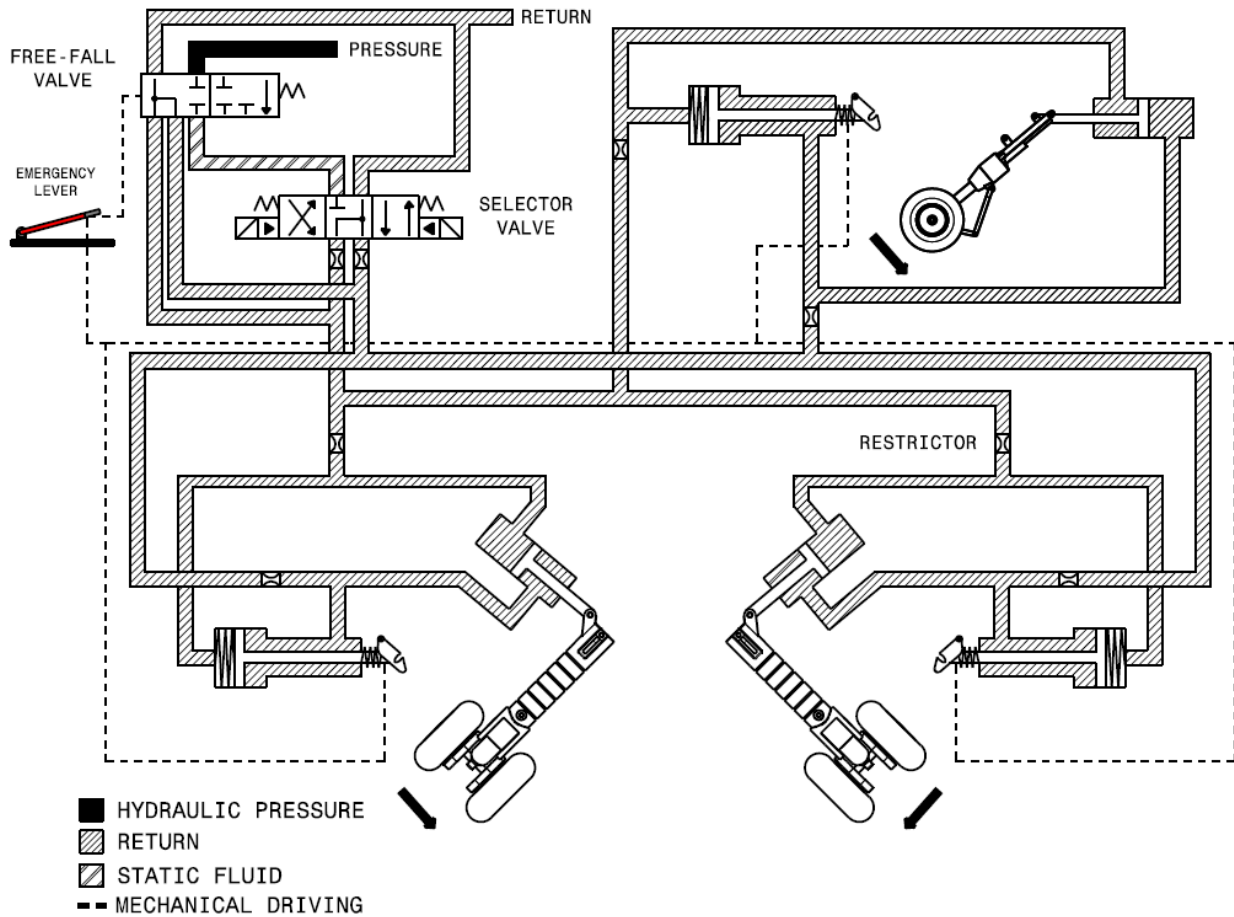


Figure 1. Free-fall system schematics considered for analysis

2. FORMULATION

The basic formulation that composes the free-fall system model will be introduced as divided into two separated topics: the hydraulic system modeling and the landing gear dynamics modeling.

2.1. Hydraulic system modeling

The landing gear associated hydraulic system is modeled applying a discrete element method, characterized by the segregation of system important behavior effects like compliance, inertance and pressure drop, as well as the isolated components presented in the system such as valves, restrictors and actuators, as discrete elements connected by means of the continuity law or specific pressure conditions.

Along the whole hydraulic system, constant values based on a nominal flight environmental condition are applied to the fluid viscosity and density, since it is expected no significant temperature variations in the system during the emergency operation. However, the fluid density also exhibits a pressure-dependence variation, whose effect can be represented together with the tubing flexibility by a discrete element called “system compliance”. The ideal compliance (C_f) is related to the fluid flow (Q) and line pressure (P) through the Eq. (1) (Doebelin, 1998).

$$C_f = \frac{A L \Delta \int Q dt}{\beta_e P} \quad (1)$$

Equation (1) also illustrates how the system compliance can be expressed in terms of the tube internal sectional area (A) and length (L) and a parameter known as the “effective bulk modulus” (β_e). In the absence of gas, the system effective bulk modulus is expressed by Eq. (2), where β_L and β_C represent the fluid and the tubing bulk modulus, respectively (Merritt, 1967).

$$\frac{1}{\beta_e} = \frac{1}{\beta_C} + \frac{1}{\beta_L} \quad (2)$$

While the fluid bulk modulus can be easily found in fluid catalogs, the tubing bulk modulus can be determined in terms of the tube inside diameter (D), the tube thickness (e) and the Modulus of Elasticity (E) and Poisson's Ratio (ν) of the tubing material, as described in Eq. (3) (Merritt, 1967).

$$\frac{1}{\beta_C} = \frac{2}{E} \left[\frac{(1+\nu)(D+2e)^2 + (1-\nu)D^2}{4e(D+e)} \right] \quad (3)$$

Due to its kinetic energy, the fluid flow exhibits another effect known as "fluid inertance". Represented as another discrete element, the pressure drop (ΔP) through the fluid inertance element is associated with the fluid flow according to Eq. (4) (Doebelin, 1998).

$$\Delta P = I_f \frac{dQ}{dt} \quad (4)$$

The value of the inertance parameter (I_f) depends on the flow regime and, thus, on the Reynolds number. Being again the tube inside diameter denoted by D , the Reynolds number (Re) is related to the fluid density (ρ), fluid dynamic viscosity (μ) and fluid velocity (V) by the Eq. (5).

$$Re = \frac{\rho V D}{\mu} \quad (5)$$

For laminar flows, that is, Reynolds numbers less than 2000, the inertance value is given by Eq. (6). On the other hand, for Reynolds numbers greater than 4000, the flow regime can be considered turbulent and the inertance parameter assumes the value provided by Eq. (7). Since between these two Reynolds number limits the flow exhibits a transitional regime, a value interpolated from both of them may be applied to I_f .

$$I_f = \frac{4\rho L}{3A} \quad (6)$$

$$I_f = \frac{\rho L}{A} \quad (7)$$

The pressure drop suffered by the fluid flowing through the tube will be modeled as another discrete element. Considering horizontal straight tubing and completely developed flow, the pressure drop along the tube can be given by a semi-empirical equation as defined in Eq. (8).

$$\Delta P = f \frac{L}{D} \frac{\rho V^2}{2} \quad (8)$$

In the right-hand side of Eq. (8), the first term is called the friction factor (f) and is dependent on tubing roughness and also on Reynolds number. For a new smooth tube, the friction factor becomes a function of just the Reynolds number, but calculated differently for laminar and turbulent flow regimes. Thus, for laminar regimes, again considered herein Reynolds numbers less than 2000 (Merritt, 1967), the friction factor is provided by Eq. (9), while for turbulent regimes the f value is calculated applying Eq. (10) (Munson et al, 2004; Merritt, 1967). In order to obtain values for transitional regimes, interpolation will be used.

$$f = \frac{64}{Re} \quad (9)$$

$$f = \frac{0.3164}{Re^{0.25}} \quad (10)$$

Besides the pressure drop existent along the tube length, there can be locally situated pressure drops provided by means of restrictors. The relation between the fluid flow and the pressure drop through a restrictor can be expressed by a non-linear equation, as shown in Eq. (11) (Merritt, 1967).

$$Q = C_D A_o \sqrt{\frac{2}{\rho} (\Delta P)} \quad (11)$$

In Eq. (11), the restrictor orifice area is denoted by the parameter A_o and the discharge coefficient by the term C_D . If the restrictor length is very small in order to consider it as a sharp-edged orifice, then 0.60 is commonly applied to the discharge coefficient value. On the other hand, if the restrictor has a considerable length, the discharge coefficient can be obtained from orifice length (L_o), orifice diameter (D_o) and the local Reynolds number (Re_o) as depicted in Eq. (12) and Eq. (13). The local Reynolds number definition is shown in Eq. (14).

$$C_D = \left[1.5 + 13.74 \left(\frac{L_o}{D_o Re_o} \right)^{1/2} \right]^{-1/2} \quad \text{for} \quad \frac{D_o Re_o}{L_o} > 50 \quad (12)$$

$$C_D = \left(2.28 + 64 \frac{L_o}{D_o Re_o} \right)^{-1/2} \quad \text{for} \quad \frac{D_o Re_o}{L_o} < 50 \quad (13)$$

$$Re_o = \frac{4\rho Q}{\mu \pi D_o} \quad (14)$$

Concerning the hydraulic system valves, the same formulation presented in Eq. (11) is applied to define the relation between fluid flow and pressure drop through their ports under the assumption of no internal leakage. However, for the valve modeling, the parameter A_o represents the port area, meanwhile the discharge coefficient (C_D) assumes the value 0.60 due to the consideration of sharp-edged port (Merritt, 1967).

Finally, the hydraulic actuators are the components that perform the connection between the hydraulic system and the landing gear mechanism. The actuators applied to the system of Fig. (1) are of double-acting, single-rod type. Considering Q_1 , P_1 and V_1 the fluid flow, pressure and volume, respectively, for one of the actuator's chambers, and Q_2 , P_2 and V_2 the same variables related to the other chamber, the continuity equation applied to the actuator yields to the formulation presented in Eq. (15) and Eq. (16). As it can be seen, internal leakage is being taken into account as linearly dependent to the pressure difference between the chambers, whose proportionality constant is given by the internal leakage coefficient (C_{ip}). In addition, the external leakage is also assumed proportional to chamber pressure by means of the external leakage coefficient (C_{ep}) (Merritt, 1967).

$$Q_1 - C_{ip}(P_1 - P_2) - C_{ep}P_1 = \frac{dV_1}{dt} + \frac{V_1}{\beta_e} \frac{dP_1}{dt} \quad (15)$$

$$C_{ip}(P_1 - P_2) - C_{ep}P_2 - Q_2 = \frac{dV_2}{dt} + \frac{V_2}{\beta_e} \frac{dP_2}{dt} \quad (16)$$

2.2. Landing gear dynamics modeling

The emergency landing gear extension is known as "free-fall" operation, since landing gear weight is the main responsible for the extension torque on that situation. Besides landing gear features like mass (m) and the distance (a) between its center of gravity and the landing gear-to-aircraft attachment (landing gear rotation axle), the weight torque is also a function of the aircraft roll angle (ϕ), aircraft pitch angle (θ) and the landing gear extension angles (α_{NLG} and α_{MLG}), even for a constant velocity vector flight. Since parameter g denotes the gravitational acceleration and the subscripts NLG and MLG are used to relate the terms to nose landing gear and main landing gear, respectively, the weight torque (T) becomes defined as in Eq. (17) and Eq. (18).

$$T_{NLG} = m_{NLG} g \cos \phi \cos(\alpha_{NLG} - \theta) a_{NLG} \quad (17)$$

$$T_{MLG} = m_{MLG} g \cos \theta \cos(\alpha_{MLG} \pm \phi) a_{MLG} \quad (18)$$

However, during the free-fall extension, the landing gear downward rotation suffers some resistant torques that end up decreasing the potential energy used by landing gear to extend. In order to simplify the model, the resistant torques will be grouped into two types: the viscous friction torque and the hydraulic actuator torque.

The viscous friction existing in the landing gear-to-aircraft attachment bearings and, moreover, the resistance provided by the extension mechanism on the landing gear movement are summarized in a term called “viscous friction torque”. Proportional to the extension velocities ($\dot{\alpha}_{NLG}$ and $\dot{\alpha}_{MLG}$) by a constant factor known as damping coefficient (B), the viscous friction torque (F) is given by Eq. (19) and Eq. (20), where the nose and main landing gear are again referred by the subscripts NLG and MLG .

$$F_{NLG} = B_{NLG} \dot{\alpha}_{NLG} \quad (19)$$

$$F_{MLG} = B_{MLG} \dot{\alpha}_{MLG} \quad (20)$$

The hydraulic actuator resistant torque is a consequence of the actuator piston movement due to the landing gear extension. Considering the piston mass and friction as negligible, the actuator force is caused by the pressure difference existing between its chambers applied to the area of each side of the piston. Being A_{p1} and A_{p2} the piston areas on each actuator chamber, the actuator force (h) is defined as in Eq. (21).

$$h = P_1 A_{p1} - P_2 A_{p2} \quad (21)$$

Therefore, the hydraulic actuator torque (H) is defined as in Eq. (22) and Eq. (23). However, the torque arms (r), as well as the piston displacements, which by the way are directly related to the actuator chamber volume variation, are functions of the landing gear extension angles. In order to obtain the relations of these two variables to the extension angles, CATIA software was used to raise the data from nose and main landing gear CAD drawings for some extension angle values and, then, a cubic polynomial regression was applied to adjust the curves.

$$H_{NLG} = h_{NLG} r_{NLG} \quad (22)$$

$$H_{MLG} = -h_{MLG} r_{MLG} \quad (23)$$

Figure 2 illustrates the torques discussed above and applied to both nose and main landing gear.

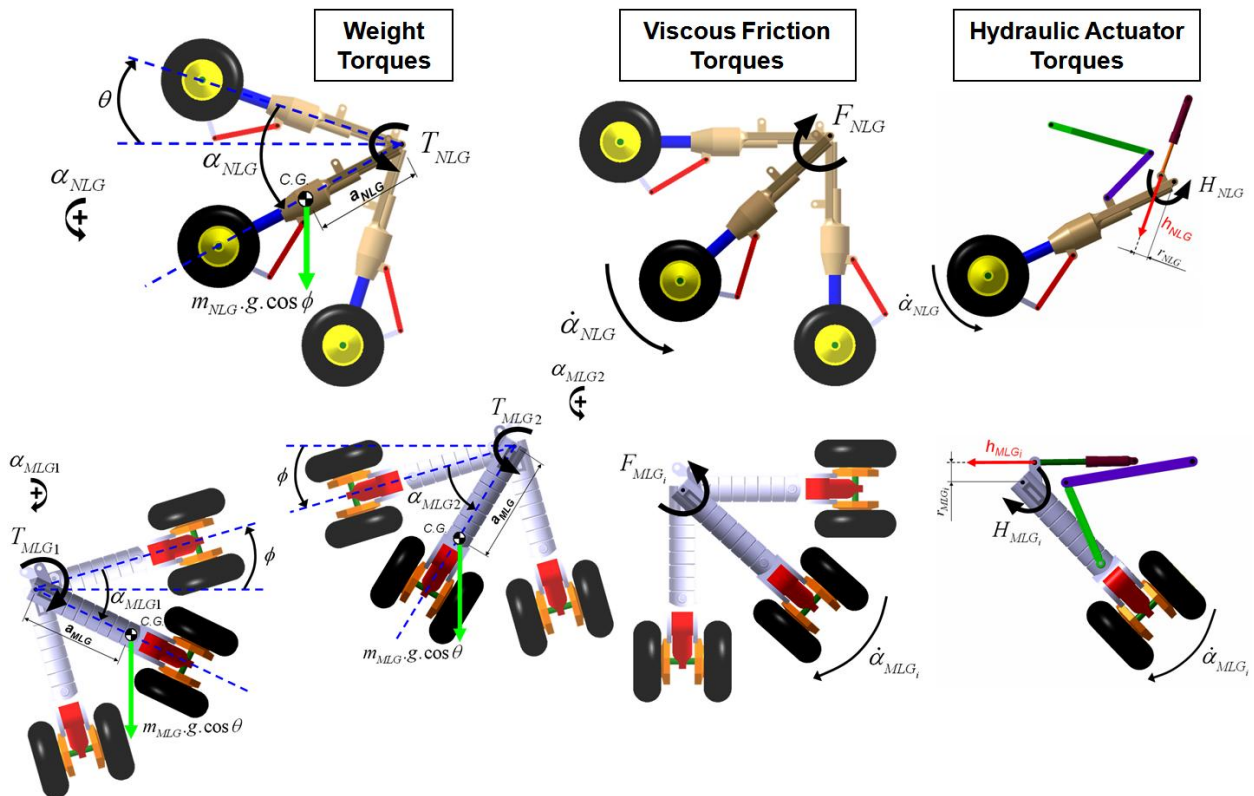


Figure 2. Weight torques, viscous friction torques and hydraulic actuator torques applied to landing gear

Finally, the aerodynamic drag can also play an important role in the landing gear emergency extension condition. Depending on the landing gear extension configuration, aerodynamic drag can offer resistance or even contribute to its movement, being this the situation for the backward extension configuration chosen for the nose landing gear of the present work. On the other hand, for a non-slip flight, no significant effect due to aerodynamic flow is noticed on the main landing gear extension, since an outboard extension configuration was selected for it.

Aiming at determining the nose landing gear aerodynamic drag, Engineering Sciences Data Unit (1987) brings a methodology to estimate its value at not very high speeds on a symmetric flight condition. This method is applicable to retractable landing gear and the final drag value is obtained from the sum of each component drag portion, taking into consideration the interference effects between them. For the drag estimation, the nose landing gear was divided into the wheels part and the structural part, being the latter compound by a cylindrical element and a rectangular element. Figure 3 depicts the nose landing gear division for drag estimation.

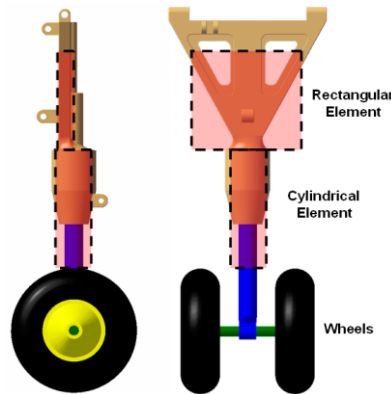


Figure 3. Nose landing gear elements division for drag estimation

The total landing gear drag (D_{NLG}) is the sum of the wheels drag (D_{wheels}), the cylindrical element drag (D_{cylind}) and the rectangular element drag ($D_{rectang}$) contributions as given in Eq. (24).

$$D_{NLG} = D_{wheels} + D_{cylind} + D_{rectang} \quad (24)$$

Basically, the components drag portions are obtained from the product of air dynamic pressure, frontal area and a particular drag coefficient. While for the cylindrical element the drag coefficient assumes an independent constant value, for wheels and rectangular element their values depend on the item geometry, as well as on the aerodynamic flow Reynolds number for the wheels drag estimation. These coefficients are taken from graphics and can be found in the reference (Engineering Sciences Data Unit, 1987).

Although the drag estimation methodology considers the landing gear stationary in the aerodynamic flow, it is being used to determine the aerodynamic drag during the landing gear extension, based on the assumption that this movement is relatively slow enough in order to allow the disregard of the non-stationary aerodynamic effects. However, the inclination of the structural components in relation to the aerodynamic flow direction must be taken into account by means of a multiplication factor.

The methodology of drag estimation also considers the presence of doors and the influence of landing gear bay on the air flow, as well as the influence of the proximity of other components in determining the drag of each element. Still, in order to simplify the aerodynamic drag estimation, most of these considerations were left out.

After defining the nose landing gear drag force, it is necessary to determine the torque this force applies during the process of landing gear extension. The landing gear exposure area and the aerodynamic drag profile on it change as the extension angle increases. Due to that, the drag torque arm has its value being constantly updated during the landing gear rotation. Thus, two different simplified drag profiles were considered for the landing gear extension process. The first profile assumes a rectangular one and it is valid for the period of time the wheels start getting outside the landing gear bay until the instant they are completely exposed to the air flow. The second one considers a triangle profile and it is applicable for the rest of the landing gear downward movement, until the time it is down and locked. Figure 4 illustrates the second profile adopted, where y_{NLG} is the distance along the landing gear of D_{NLG} to the top end of drag profile at the aircraft boundary, d_{NLG} is the drag profile length along landing gear and, finally, G_{NLG} is the aerodynamic drag torque.

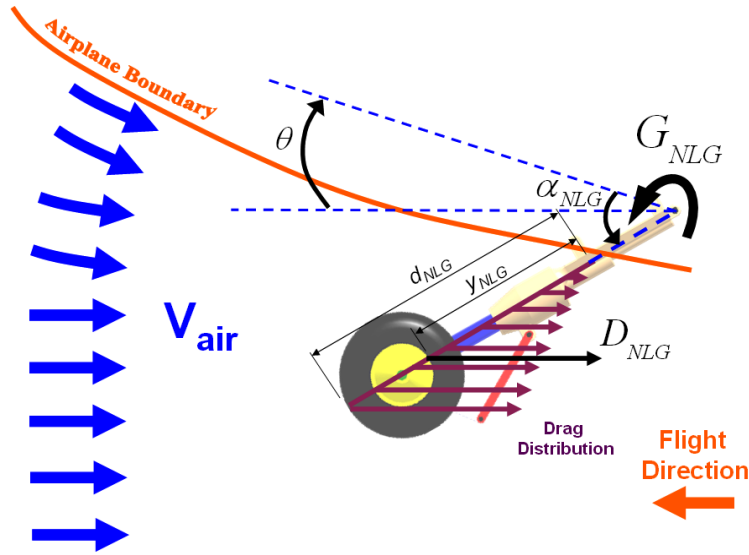


Figure 4. Aerodynamic drag profile considered for the longest landing gear extension phase

Consequently, the nose landing gear aerodynamic drag torque assumes three distinct values depending on the extension angle. For nose landing gear extension angle less than α_{NLG1} , where α_{NLG1} is the extension angle associated to the instant the landing gear wheels reach the aircraft boundary, there is no landing gear exposure to the air flow and thus drag torque is null. However, as the landing gear falls, the first components to be exposed to the aerodynamic flow comprise the wheels. For that reason, the drag force can be assumed as consisting of only the wheels drag portion, for the extension angle varying from α_{NLG1} to α_{NLG2} , being the later the extension angle value when the wheels are completely outside the landing gear bay. Using trigonometric calculations, the aerodynamic drag torque can be approximated for this extension angle range according to Eq. (25), where l_{NLG} is the landing gear length from the rotation axle to the wheels axle and d_{wheels} is the wheel diameter.

$$G_{NLG} = D_{NLG} \left[l_{NLG} \alpha_{NLG1} + \frac{d_{wheels}}{2} \left(1 + \frac{\alpha_{NLG} - \alpha_{NLG1}}{\alpha_{NLG2} - \alpha_{NLG1}} \right) \right] \quad (25)$$

For nose landing gear extension angle greater than α_{NLG2} , the drag profile of Fig. 4 is considered and the aerodynamic drag torque can be approximated by Eq. (26), where α is the airplane angle of attack. The parameters d_{NLG} and y_{NLG} , whose definitions are shown in Fig. 4, are obtained from Eq. (27) and Eq. (28), respectively. In Eq. (27), the terms l_{cylind} and $l_{rectang}$ represent the length of the cylindrical and rectangular elements of the landing gear structural part.

$$G_{NLG} = D_{NLG} \left[l_{NLG} + \frac{d_{wheels}}{2} - d_{NLG} + y_{NLG} \right] \text{sen}(\alpha_{NLG} - \alpha) \quad (26)$$

$$d_{NLG} = d_{wheels} + l_{cylind} + \frac{l_{rectang}}{1 - \cos(\pi/2 - \alpha_{NLG2})} \left[1 - \frac{\cos(\pi/2 - \alpha_{NLG2})}{\cos(\pi/2 - \alpha_{NLG})} \right] \quad (27)$$

$$y_{NLG} = \frac{2}{3} d_{NLG} \quad (28)$$

Once defined all the torques that act on the landing gear free-fall extension, they must be combined in order to satisfy the Newton's second law for rotational movement. Being I_{NLG} and I_{MLG} the moment of inertia of nose landing gear and main landing gear, respectively, thus Newton's second law applied to them results in Eq. (29) and Eq. (30).

$$T_{NLG} - F_{NLG} + G_{NLG} + H_{NLG} = I_{NLG} \ddot{\alpha}_{NLG} \quad (29)$$

$$T_{MLG} - F_{MLG} + H_{MLG} = I_{MLG} \ddot{\alpha}_{MLG} \quad (30)$$

3. MODELING

The block diagram of the free-fall system is presented in Fig. 5. As it can be seen, both right and left main landing gear were considered having the same hydraulic and landing gear physical parameters.

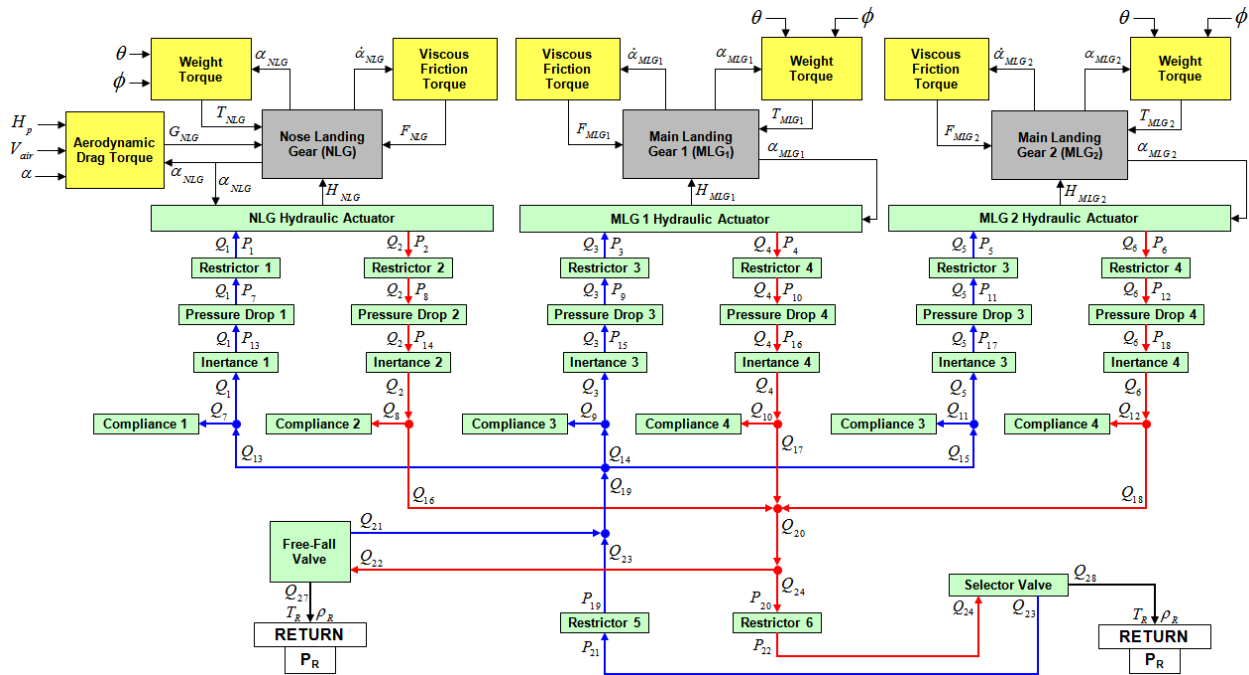


Figure 5. Free-fall system block diagram

The model external inputs comprise two flight conditions, which are the flight speed (V_{air}) and flight altitude (H_p), and some aircraft angles, like the roll (ϕ) and pitch (θ) angles, as well as the aircraft angle of attack (α). Hydraulic fluid reservoir pressure (P_R) basically represents the unique model boundary condition. In addition, the fluid reservoir density (ρ_R), calculated at the reservoir temperature (T_R), is the one applied throughout the hydraulic system.

Regarding the landing gear down locking criterion, since the down lock mechanism was not modeled, it is assumed that, at an extension angle of 89° (1.533 radians), the landing gear is instantaneously locked supposedly by means of a mechanical lock, which brings it immediately to the final extension angle of 90° ($\pi/2$ radians). In practice, down locking angles even less than 89° (1.533 radians) may be observed, which makes adopted criterion satisfactory.

4. SIMULATION RESULTS

In order to simulate the free-fall system presented in Fig. 5, a MATLAB Simulink model was created. Applying a variable-step algorithm based on a Runge-Kutta (4,5) explicit method known as “ode45”, the model was simulated using the parameters nominal values. After the simulation, variables like hydraulic pressure and fluid flow at the tubes, as well as the landing gear extension angles and velocities, were plotted and analyzed.

Below, it is presented the development of the landing gear downward movement over the time. The landing gear extension angles are shown in Fig. 6, while landing gear extension velocities are presented in Fig. 7.

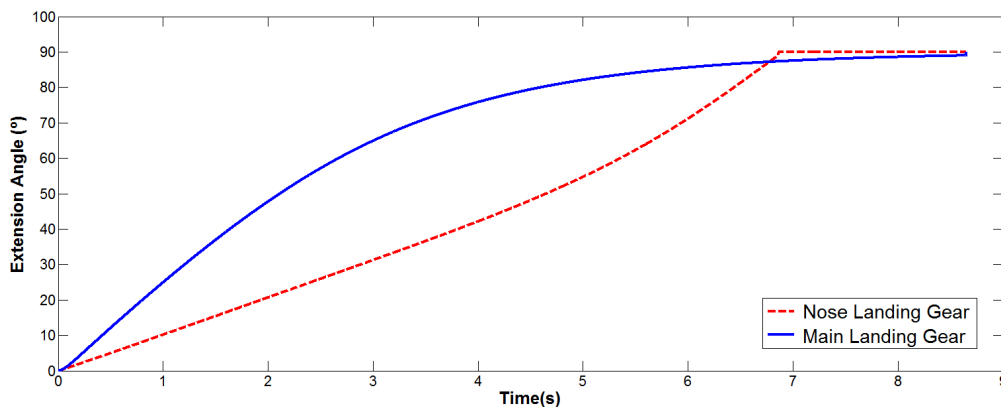


Figure 6. Landing gear extension angles for nominal free-fall operation

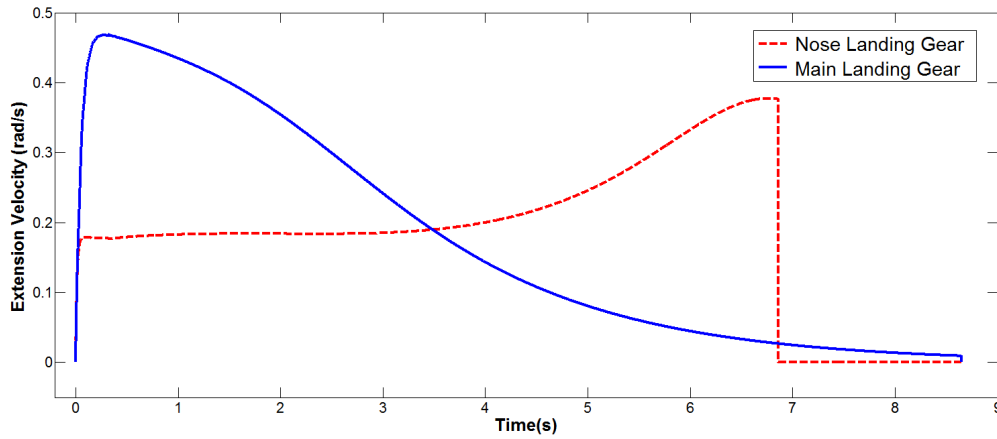


Figure 7. Landing gear extension velocities for nominal free-fall operation

As it can be seen, the nose landing gear takes 6.86 seconds to extend by free-fall, while the main landing gear takes a little more, that is, 8.65 seconds.

5. MODEL OPTIMIZATION

The landing gear extension behavior described in Fig. 6 and Fig. 7 represents a typical description of what can be found for many aircrafts in terms of free-fall operation. While the nose landing gear reaches the lowest point with a considerable amount of kinetic energy, the main landing gear hardly gets down and locked due to the small kinetic energy it has at the end of its movement. Because of that, an optimization process can be applied to the model in order to better adjust each landing gear kinetic energy level, so that any damage to airplane structure is avoided (damping optimization) meanwhile both landing gear certainly get down and locked. Since the landing gear final position is virtually the same for normal flight conditions, the potential energy was not taken into account.

The Simulink Response Optimization library, by means of the “Signal Constraint Block”, allows the user to define some limits to the model outputs and optimize the variable response in order to better obey these bounds (The Mathworks Inc., 2007). Thus, the nose landing gear down locking kinetic energy adjustment was chosen with the purpose of demonstrating an optimization process. This way, the kinetic energy output (K_{NLG}) as defined in Eq. (31) had its final value (close to the down position) limited by lower and upper bounds, as well as by a lateral bound that imposed a limiting time for the nose landing gear to extend.

$$K_{NLG} = \frac{1}{2} I_{NLG} (\dot{\alpha}_{NLG})^2 \quad (31)$$

The parameters selected to have their values changed during the optimization process were restrictor 1 diameter (D_{o1}) and restrictor 2 diameter (D_{o2}). The restrictors are placed adjacent to the nose landing gear hydraulic actuator, in such a way that restrictor 1 is in the extending line and restrictor 2 is in the retraction line of the hydraulic system.

Finally, applying the default optimization algorithm (gradient descent) and model size (medium scale) of the “Signal Constraint Block”, the optimum values of both diameters were achieved. Table 1 exhibits the limiting, initial guesses and optimized values of the two parameters evaluated.

Table 1. Limiting values, initial guesses and final values of the parameters evaluated during the nose landing gear kinetic energy optimization.

Parameter	Description	Initial Guess	Minimum Value	Maximum Value	Optimized Value
D_{o1}	Restrictor 1 Orifice Diameter	3.2×10^{-3} m	5.0×10^{-4} m	4.0×10^{-3} m	5.5275×10^{-4} m
D_{o2}	Restrictor 2 Orifice Diameter	3.2×10^{-3} m	5.0×10^{-4} m	4.0×10^{-3} m	5.5275×10^{-4} m

Figure 8 illustrates the kinetic energy level during the nose landing gear extension movement for the optimization process iterations. As it can be seen, the final output solution fits properly within the limits initially defined in order to assure an acceptable landing gear free-fall behavior. A reduction of 11.7% on down locking kinetic energy level was possible.

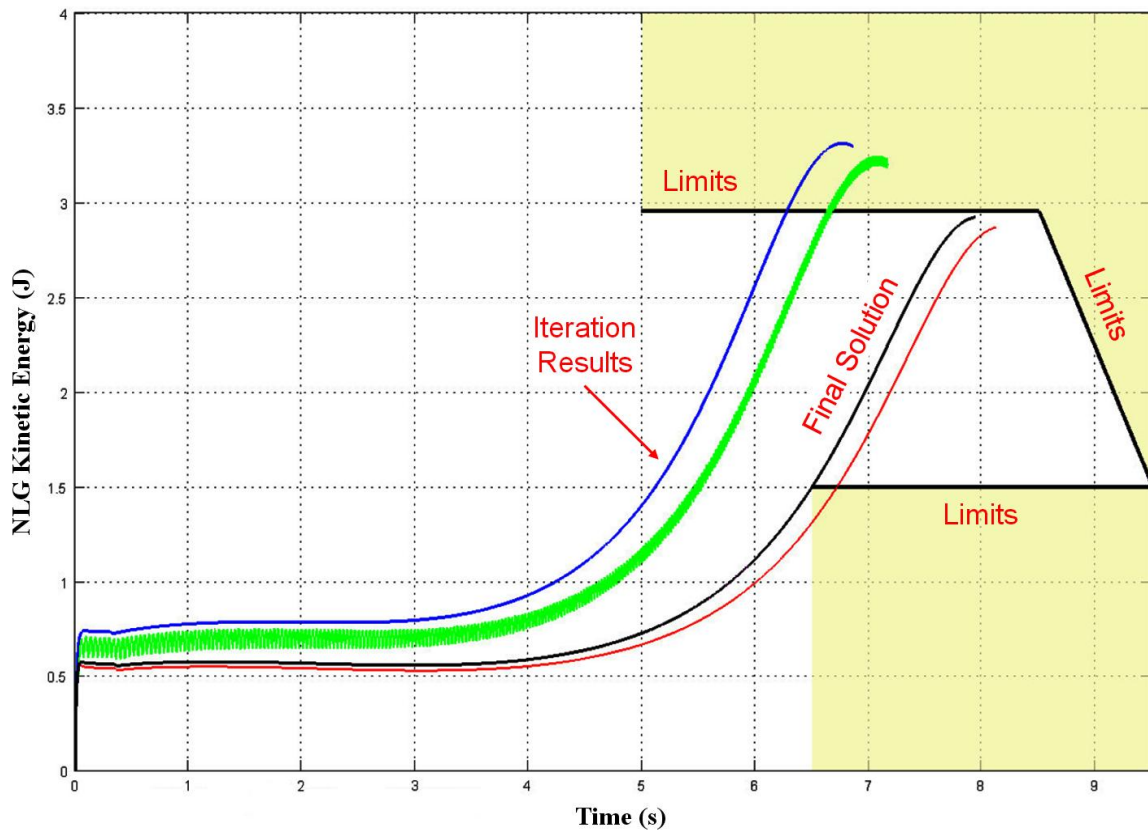


Figure 8. Nose landing gear kinetic energy optimization process

6. CONCLUSIONS

Involving a wide variety of engineering subjects, the landing gear free-fall operation modeling consisted in a challenging task. In spite of the assumptions considered, the formulation applied to construct the model seemed to be satisfactorily representative of an airplane landing gear common free-fall extension operation.

In addition, the optimization process applied to nose landing gear kinetic energy demonstrated that the free-fall operation, notwithstanding the simplicity the system constructive configuration may exhibit, could be improved by means of a properly adjustment of the related system parameters values. Although more complex and laboring, an optimization process taking into account a greater quantity of system parameters might have led to a better extension-by-gravity performance not only for the nose landing gear, but for the main landing gear too. However, it is important to mention that cost, weight and manufacturing issues should always be considered over the accomplishment of any system design optimization.

7. ACKNOWLEDGMENTS

Special thanks to EMBRAER and ITA/FCMF for all the support and facilities provided.

8. REFERENCES

- Currey, N.S., 1998, "Aircraft Landing Gear Design: Principles and Practices", AIAA Education Series, Washington, USA, 373 p.
- Doebelin, E.O., 1998, "System Dynamics: Modeling, Analysis, Simulation, Design", Marcel Dekker, New York, USA, pp. 54-75, 206-255.
- Engineering Sciences Data Unit, 1987, "Undercarriage Drag Prediction Methods", ESDU 79015, ESDU International, London, England, 39 p.
- The Mathworks Inc, 2007, "Matlab: the language of technical computing", Natick, USA.
- Merritt, H.E., 1967, "Hydraulic Control Systems", John Wiley & Sons Inc., New York, USA, 358 p.
- Munson, B.R., Young, D.F. and Okiishi, T.H., 2004, "Fundamentals of Fluid Mechanics", 4th edition, Edgard Blücher, São Paulo, Brazil, pp. 398-400, 409-415, 425-431.

9. RESPONSIBILITY NOTICE

The authors are the only responsible for the printed material included in this paper.